Simulation of the aerosol optical depth over Europe for August 1997 and a comparison with observations

A. Jeuken[1] and J. P. Veefkind

Royal Netherlands Meteorological Institute, De Bilt, The Netherlands

F. Dentener and S. Metzger

Institute for Marine and Atmospheric Research Utrecht (IMAU), Utrecht, The Netherlands

C. Robles Gonzalez

TNO Physics and Electronics Laboratory, The Hague, The Netherlands

Abstract. A chemical transport model has been extended with an aerosol model describing processes which determine the mass distribution of sulfate, nitrate, ammonium, and aerosol associated water. A specific summer episode is simulated, and the results have been compared to surface concentration measurements and with the aerosol optical depth (AOD) retrieved from satellite measurements, with a focus on the European continent. This study is one of the first to use satellite retrievals over land for this purpose. An average difference in AOD between model and satellite measurements of 0.17-0.19 is calculated, and on average only 40-50% of the observed satellite signal can be explained by our modeled aerosol. In contrast, the observed patterns of optical thickness are well simulated by the model. Also, surface concentrations of simulated aerosol components are in close agreement with measurements. Errors in the vertical distribution of sulfate, ammonium, and nitrate, and hence in the vertical distribution of hygroscopic growth, and errors in modeled optical parameters may partly account for the observed differences in AOD. However, we argue that the most important reason for the large difference is due to the fact that organic and mineral aerosol are not taken into account in this model simulation. A sensitivity study with reduced SO_2 emissions in Europe showed that reduction of the emissions of SO_2 in the model leads to a better agreement with surface measurements of SO_2; however, calculated sulfate was less strongly influenced.

1. Introduction

Atmospheric aerosol particles play an important role in the global radiation budget, either directly by scattering and absorbing solar radiation or indirectly, by influencing the microphysical properties of clouds [e.g., *Charlson et.al.*, 1992; *Chuang and Penner*, 1995]. Anthropogenic emissions of aerosols and aerosol precursors have increased rapidly over the last century. Whereas over the last two decades there has been a decrease in Europe and the United States, emissions are still increasing in other parts in the world, like for example China and India. It is therefore important that accu-

rate chemistry transport and climate models are being developed to simulate the large variety of aerosol sources, sinks, concentrations and optical properties in the present and future.

Langner and Rodhe [1991] were among the first to perform a global three-dimensional simulation of sulfate aerosols, and since then more model studies were devoted to improve the accuracy of sulfate simulations [e.g., *Pham et al.*, 1995; *Feichter et al.*, 1996; *Chin et al.*, 1996; *Roelofs et al.*, 1998]. Also, for other aerosol species like organic aerosols [*Liousse et al.*, 1996], black carbon [*Cooke and Wilson*, 1996], dust aerosols [*Tegen and Fung*, 1994; *Guelle et al.*, 2000], sea-salt aerosol [*Gong et al.*, 1997], and nitrate aerosols [*Metzger et al.*, 1999; *Adams et al.*, 1999], three-dimensional model studies have become available. For sulfate aerosols the confidence in model results is largest. Model results for other aerosol components indicate large uncertainties, a large part of which can be attributed to the lack of measurements available for validation. However, it

---

[1] Also at Eindhoven University of Technology, Eindhoven, The Netherlands.

is important to notice that the modeling of the sulfur cycle is still associated with large uncertainties.

Sulfate aerosols vary strongly both spatially and temporarily. The main reasons for this variation are the irregularly spaced sources of the sulfate precursor SO_2 and the strong dependence of SO_2 oxidation and aerosol scavenging on cloud and precipitation processes. The distribution of SO_2, in addition, strongly depends on dry deposition at the surface, since the deposition velocities vary considerably depending on surface characteristics and local meteorology. As a result, the lifetime of SO_2 and sulfate is short (1-2 and 3-5 days, respectively). The large variability of the sulfur species poses stringent requirements on the model. Owing to a limited resolution and owing to rather crude parameterizations of the "wet" processes, current models have difficulties simulating the observed variability of sulfate correctly. From the Comparison of Large Scale Atmospheric Sulfate Aerosol Models (COSAM) workshop [Barrie et al., 2001; Lohmann et al., 2001; Roelofs et al., 2001], in which about 10 global models participated, it was concluded that the variation in results for sulfur components among the different models is large. Most of the differences originate from the treatment of cloud and precipitation processes. Model results for sulfate are on average within 20% of the observed concentrations at remote sites, while SO_2 is overestimated by as much as a factor of 2.

Measurements [EMEP, 1998; Ten Brink et al., 1996a] indicate that, at least in Europe, nitrate aerosol may constitute an important mass fraction of the aerosol, and that therefore simulations of the sulfur cycle alone may not always be sufficient to obtain the aerosol properties needed to calculate the radiative forcing. However, the aerosol optical properties also strongly depend on the hygroscopicity (aerosol associated water), which in turn depends on the composition of the aerosol. The latter is difficult to model in a global model, since species such as ammonium and nitrate, are volatile and partition between gas and aerosol phase. The gas-aerosol partitioning strongly depends on the ambient relative humidity and temperature, on the availability of aerosol precursor gases (HNO_3, NH_3) and the preexistence of aerosol particles. The model described in this paper therefore includes a simplified thermodynamical aerosol equilibrium model [Metzger, 2000] to calculate the nitrate aerosol mass and the amount of water contained in aerosols.

Unfortunately, there is a severe lack of measurements to validate global aerosol model simulations. Especially information about the vertical distribution is lacking [e.g., Lohmann et al., 2001; Guelle et al., 1998b]. Ground-based experiments can provide detailed information on the aerosol size distribution and chemical composition. However, most of these measurements are point measurements near the surface, and may not be representative for the aerosol throughout the boundary layer and free troposphere. Aircraft observations are expensive and therefore not suitable for long-term

monitoring. Satellite remote sensing on the other hand can provide daily measurements of column integrated aerosol properties, such as the spectral aerosol optical depth (AOD), on spatial scales ranging from a few kilometers to global. The spectral AOD potentially holds information on the aerosol load and on the aerosol size distribution [Tanré et al., 1996], and limited information can be derived on the chemical composition. The disadvantages of present satellite remote sensing measurements are the lack of profile information, and the relatively large time span (usually more than 24 hours) between two successive satellite overpasses over an area. Combination of aerosol satellite remote sensing and transport modeling can be applied for interpretation of spatial aerosol distributions, as observed from the satellite.

In this paper the AOD at 0.555 μm derived from the Along Track Scanning Radiometer 2 (ATSR-2) on board the European ERS-2 satellite is compared with AOD calculations from the chemistry transport model TM3. In contrast with previous studies which have focused on satellite measurements over the ocean away from major sources [e.g., Tegen et al., 1997; Haywood et al., 1997], we focus on the much more complex situation over land. The comparison is made for a case study over Europe, for August 1997. For this month a complete data set containing all ERS-2 overpasses over Europe published by Robles-Gonzalez et al. [2000], has become available. Unfortunately up to now no other complete month of the ATSR-2 derived AOD for Europe has been made available. The weather situation for August 1997 is characterized by cloud-free conditions over most of Europe and is therefore ideal for retrieving aerosol information from satellite measurements. The total AOD is estimated from the column burden of the sum of simulated sulfate, nitrate, and aerosol associated water. Since it is well known from measurements [Ten Brink et al., 1996b] that a significant fraction of the aerosol consists of other components, e.g., carbonaceous or sea-salt aerosol, we concentrate on spatial patterns rather than absolute values of AOD. The purpose is to investigate to what extent the AOD, calculated from nitrate, sulfate and the aerosol associated water mass can explain the observed spatial patterns in AOD over Europe. Before comparing the column-integrated AOD, we first compare the day-to-day variability of aerosol species with surface concentration measurements. As opposed to the bulk aerosol column comparison, in this way each model simulated aerosol component is evaluated using independent measurements. Two model simulations with two different emission scenarios are used in the comparison.

2. Model Description

2.1. Transport Processes

The TM3 off-line chemistry transport model has gradually evolved from the TM2 model as developed by Heimann [1995] at the end of the eighties. Three-

dimensional tracer transport in the model is accounted for by advection for the resolved motions and by convection and vertical diffusion for the unresolved motions (the sub grid-scale). The advection of tracers in the model is calculated with the slopes scheme of *Russell and Lerner* [1981]. The sub grid-scale convection fluxes are calculated using the scheme of *Tiedtke* [1989].

A new boundary layer scheme similar to the scheme used in the ECMWF model [*Beljaars and Viterbo*, 1998] has been implemented. For stable atmospheric conditions we use a local formulation based on the work of *Louis et al.* [1982] and for unstable conditions we use a nonlocal formulation based on the work of *Holtslag and Boville* [1993]. In addition, the time resolution of the meteorological input has been increased from 6 to 3 hours. This new vertical diffusion scheme has been tested in TM3, by comparing surface and profile measurements of the radio nuclide radon (^{222}Rn) with model output [*Jeuken*, 2000]. It was concluded that mainly due to the better temporal resolution the diurnal cycle in radon surface concentrations is much better resolved by the model and that improvement has been achieved compared to earlier simulations by *Dentener et al.* [1999]. Absolute concentrations are, however, still somewhat overestimated by the model indicating that mixing remains somewhat underestimated [see also *Dentener et al.*, 1999]. The current horizontal resolution of the model is 2.5° by 2.5° , and there are 31 layers in the vertical between the surface and 10 hPa.

2.2. Chemistry

The chemical and physical processes leading to the formation of sulfate, ammonium and nitrate have been modeled and coupled to the chemistry version of TM3 as described by *Houweling et al.* [1998]. This chemistry model describes the background tropospheric CH_4-O_3-HO_x-NO_x chemistry and the chemistry of nonmethane hydrocarbons (NMHCs), using a modified version of the widely used Carbon Bond mechanism [*Gery et al.*, 1989]. To calculate photolysis rates, we use the scheme adapted from *Krol and Van Weele* [1997] consistently with local cloud cover and ozone columns [*Lelieveld and Dentener*, 2000]. We have added the gas and cloud phase reactions of SO_2, DMS, NH_3, SO_4^{2-}, and NH_4^+ [*Dentener and Crutzen*, 1994; *Pham et al.*, 1995].

Dissociation and in-cloud reaction rates are pH-dependent. Ignoring the contribution of weak acids and bases the pH is calculated from the strong acids and bases as $[H^+]=2[SO_4^{2-}]_a+[MSA]_a-[NH_4^+]_a+[HNO_3]_g+[NO_3^-]_a$, where subscripts a and g stand for dissolved aerosol and gaseous species, respectively. For pH>4.3 the dissociation of the weak acids SO_2 and CO_2 as well as the base NH_3 are taken into account.

To be able to calculate the gas-aerosol partitioning of the ammonia-sulfate-nitrate system, we have added a simplified thermo-dynamical equilibrium model (EQM) to TM3 [*Metzger*, 2000]. The EQM describes the equilibrium partitioning between aerosol precursor gases

(NH_3, H_2SO_4, HNO_3, and HCl) and liquid and solid aerosol phases for major inorganic aerosols compounds (ammonium, sulfate, nitrate, sea-salt, mineral dust). Usually EQMs are complex models in which the activity coefficients need to be calculated iteratively [e.g., *Nenes et al.*, 1998] and therefore demand exhaustive amounts of computing resources. An alternative noniterative parameterization has been introduced, that allows to calculate the gas-aerosol partitioning for global modeling rapidly and accurately. The method is based on the fact that, for atmospheric aerosols in thermodynamical equilibrium with the ambient air, the solute activity, and hence the activity coefficient calculation, is governed by the aerosol associated water. The latter depends only on the relative humidity and the type and number of moles of dissolved matter. Central to the method is the use of concentration domains, which are based on the mole ratio of the solute concentrations. For instance, the aerosol can be in the "sulfate-rich" domain (i.e., $2NH_4^+ < SO_4^{2-}$) or in the sulfate poor case (i.e., $NH_4^+ > SO_4^{2-}$). On the basis of the domain and the relative humidity, the aerosol associated water amount can be calculated and from this it is possible to derive directly the activity coefficients using a generalization of Raoult's law. The activity coefficients calculated non-iteratively with the new method compare well with those obtained with common iterative methods of various EQMs [*Metzger*, 2000]. In the version of the EQM used in this paper, the thermodynamic properties as used in the recent state-of-the-art EQM Isorropia [*Nenes et al.*, 1998] are used. It was shown by *Metzger* [2000] that results are generally very close to those obtained by Isorropia and well within the range of results obtained with other EQMs.

2.3. Wet Deposition

In our model we consider two types of precipitation: large scale or synoptic precipitation and convective precipitation. Generation of synoptic precipitation is calculated in TM3 itself, using the same formulations as in the operational ECMWF weather forcast model [*Tiedtke*, 1993] and the ECMWF diagnosed relative humidity, cloud liquid, and ice content. In-cloud scavenging of gases and aerosols is calculated according to these local precipitation rates using a first-order loss approach [e.g., *Guelle et al.*, 1998a]. HNO_3 is assumed to be a completely soluble gas and is scavenged in a cloud at the same rate as the conversion of cloud water into precipitation. The scavenging rate for any other gaseous species is scaled to the scavenging rate of HNO_3 according to its Henry equilibrium constant [*Dentener and Crutzen*, 1993]. Below cloud scavenging of gases is calculated as a function of the mass transfer coefficient, the dimensionless rain liquid water content and the rain droplet radius [*Roelofs and Lelieveld*, 1995].

For below cloud scavenging of accumulation mode aerosols we adopt a scavenging efficiency of 0.05 mm^{-1}, taken from *Dana and Hales* [1991], for a lognormal

background aerosol distribution with modal parameters $r=0.13$ μm and $\sigma=1.9$ [Jaenicke, 1988] and a frontal rain spectrum with a geometric mean radius R_g of 0.02 cm with $\sigma=1.86$. It should be noted that the aerosol below cloud scavenging coefficient is strongly dependent on the actual choice of r and σ, but in any case rather slow as compared to in-cloud scavenging.

For below-cloud scavenging of SO_2 we assume that the maximum scavenging rate (the rate of HNO_3 scavenging) is only limited by the amount of H_2O_2 in the falling rain with a pH below 5 assuming fast reaction of H_2O_2 and $S(IV)$. Above pH=5 the below-cloud scavenging rate of SO_2 is equal to the scavenging rate of HNO_3, assuming that oxidation by O_3 effectively removes $S(IV)$ in rain. By keeping track of the amount of H_2O_2 and H^+ scavenged in the grid cells above, the below cloud scavenging rate of SO_2 is calculated. This simplified method probably presents an upper limit for the below cloud scavenging of SO_2 since it assumes that the reactions are fast compared to the timescales of existence of rain droplets.

The removal of tracers in convective clouds has been parameterized as a function of the updraft mass flux [Balkanski et al. 1993]. In this method scavenging is directly coupled to the intensity of convection assuming 100% efficiency for deep and 50% for shallow (precipitating) convective clouds.

2.4. Dry Deposition

Dry deposition is the major sink for soluble or reactive trace gases like SO_2 and NH_3. Especially in wintertime when low H_2O_2 concentrations limit SO_2 oxidation it will be the dominant sink for SO_2. Therefore we use the detailed dry deposition scheme as described by Ganzeveld et al. [1998]. In this scheme the deposition velocity is calculated from the aerodynamic resistance, the quasi-laminar boundary layer resistance and the surface resistance. The surface resistance of SO_2 strongly depends on snow cover and surface wetness. For sulfate aerosol the deposition velocity is dependent on two parameterized aerosol size distributions, one for land and one for oceans, and further depends on the wind velocity, which may increase the contact surface area when the sea becomes rough. Most meteorological surface fields for example in the aerodynamic resistance are calculated from ECMWF meteorological data. Vegetation descriptions are derived from a global ecosystem database [Olson et al., 1983]. Variables like snow cover and surface wetness are prescribed by ECHAM4 climatological data [Claussen et al., 1994].

2.5. Emissions

Anthropogenic emissions of NO_x, NH_3, SO_2 have been taken from the historical Emission Database for Global Atmospheric Research (EDGAR) [Olivier, 1996; Bouwman et al., 1997] calculated on a grid of 1° by 1°. Van Aardenne et al. (A high resolution data set

of historical anthropogenic trace gas emissions for the period 1890-1990, submitted to Global Biogeochemical Cycles, 2000) have estimated trends in these emissions, based upon demographical, economical, agricultural, and technological developments during the past century. The time resolution of the database is 10 years until 1970 and 5 years hereafter until 1990. For 1997, which is the year of interest, we have extrapolated the 1990 emission data based on energy consumption statistics. The seasonal variation in NO_x and SO_2 is based upon the Global Emission Inventory Activity (GEIA) database valid for 1985 [Benkovitz et al., 1996]. Volcanic sulfur emissions are estimated by Andres and Kasgnoc [1998]. DMS emissions are obtained by combining the oceanic surface concentrations compiled by Kettle et al. [1999] with turbulent air-sea exchange coefficient calculated by using the parameterization by Liss and Merlivat [1986]. For DMS land emissions and SO_2 natural emissions we use the estimates of Spiro et al. [1992]. All other emissions are described in Houweling et al. [1998]. To investigate the influence of differences in SO_2 emissions on the sulfur budget we alternatively use SO_2 emissions from the Core Inventory Air (CORINAIR) project. In contrast with the global EDGAR data after 1990, reported CORINAIR emissions take into account the changes in emission factors, e.g., changes in the conversion factors from fossil fuel use by electric power generation to SO_2 emissions. While the total of SO_2 emissions for Europe in the extrapolated EDGAR database is 22 Tg S, it is only 12 Tg S in the CORINAIR database. For other regions it is expected that differences between the extrapolated EDGAR and other independent inventories are less; e.g., in North America where major emission reductions took place before 1990. Both databases will be used in section 5 to demonstrate the effect of changing emissions on aerosol formation.

2.6. Budgets

In order to illustrate the magnitude of processes and to be able to compare our model with other published models, we calculate the annual and global budgets of SO_2, sulfate, nitrate, and ammonium for the year 1997. Table 1 shows that the turnover times of SO_2 and SO_4^{2-} are both relatively short, compared to other global sulfur models. In the COSAM [Barrie et al., 2001] intercomparison the turnover time was in the range 1.3-3.1 days for SO_2 and 3.6-7.5 days for SO_4^{2-}. So, especially for sulfate, TM3 is in the low end of the range (of 10 models). This short turnover time of sulfate is likely due to the effective wet scavenging, which as we noticed from tests with ^{210}Pb [Jeuken, 2000] somewhat overestimates the removal of accumulation mode aerosol by in-cloud scavenging. The low turnover time of SO_2 can be explained by a rather effective below cloud scavenging, which is completely ignored in most other models.

Table 2 shows the anual and global budgets of the nitrogen containing aerosol species. Nitrate clearly consti-

Table 1. Annual budget for SO_2 and SO_4^{2-} for the Year 1997.[a]

	Global		NH		NH-PBL	
	SO_2	SO_4^{2-}	SO_2	SO_4^{2-}	SO_2	SO_4^{2-}
Emission	(2540)	(58)	(2213)	(52)	(2090)	(52)
Dry deposition	1150	100	1042	75	1042	75
Wet deposition	916	982	633	738	486	424
SO_2+OH	254	(254)	210	(210)	158	(158)
SO_2+O_3/H_2O_2	770	(770)	545	(545)	293	(293)
Burden	12.9	9.94	11.3	7.2	6.5	3.3
Turnover time, day	1.52	3.36	1.69	3.23	nd	nd

[a]Units are in 10^9 moles yr^{-1}. The oxidation of DMS by OH and NO_3 serves as an additional source for SO_2 of about 550×10^9 mole yr^{-1}. Source terms are marked in parentheses. "nd" means that the budget has not been determined, because of the missing transport terms in the nonglobal budgets. However, we have assumed interhemispheric transport to be negligible.

tutes the smallest fraction of the aerosol. Expressed in mass, sulfate contributes on average 65%, ammonium 21%, and nitrate 14% to the global simulated aerosol burden of about 1.5 Tg. In the work of *Adams et al.* [1999] the total aerosol burden of sulfate + nitrate + ammonium (excluding the water fraction) was calculated to be 2.6 Tg of which sulfate constitutes 80%, ammonium 15% and nitrate 5% only. So, in comparison, we find a 50% lower sulfate burden and a slightly higher nitrate burden. Differences in the sulfate burden are likely due to differences in oxidation chemistry and removal processes. In addition our study used a much higher horizontal and vertical resolution than *Adams et al.* [1999] which certainly can explain some differences. Furthermore, the on-line consideration of particulate NO_3^- and HNO_3 in our model, compared to the off-line approach employed by Adams, results in a higher nitrate aerosol burden in our model due to the different removal efficiency by dry deposition of particulate and gas phase nitrate. High concurrent NO_x and NH_3

emissions over southeast Asia and India in combination with rapid vertical transport around the Himalayas result in a rather long-living nitrate-aerosol in the upper troposphere. This upper tropospheric plume is responsible for the relatively long global average turnover time of 3 days shown in Table and has also been previously calculated by *Adams et al.*, [1999]; and *Metzger* [2000]. Unfortunately, to our knowledge, there are no measurements to confirm the existence of such a high nitrate layer in the upper troposphere.

3. Modeling the Aerosol Optical Depth

The TM3 model computes the spatial and temporal distribution of the mass of sulfate and nitrate aerosol in various degrees of neutralization by ammonium. To derive the aerosol optical depth (AOD) of the sulfate/nitrate/ammonium aerosol, assumptions have to be made on the aerosol size distribution. Other aerosol components, such as carbonaceous aerosols may also

Table 2. Annual budget for SO_2 and SO_4^{2-} for the Year 1997.[a]

	Global			NH			NH-PBL		
	NH_3	NH_4^+	NO_3^-	NH_3	NH_4^+	NO_3^-	NH_3	NH_4^+	NO_3^-
Emission	(3710)	na	na	(3030)	na	na	(3030)	na	na
Dry deposition	1380	214	6	1229	179	6	1229	179	6
Wet deposition	685	1360	202	488	1095	185	404	644	110
NH_3+OH	68	na	na	51	na	na	34	na	na
$NH_{3aq} + SO_4^{2-}{}_{aq}$	489	(489)	na	297	(297)	na	217	(217)	na
$NH_{xae} + HNO_{3ae}$	208	(208)	(208)	nd	nd	nd	nd	nd	nd
$NH_{xae} + H_2SO_{4ae}$	880	(880)	na	nd	nd	nd	nd	nd	nd
Burden	9.23	17.3	3.19	6.76	13.6	2.72	4.63	6.12	1.30
Turnover time, day	0.91	4.01	5.60	0.81	nd	nd	nd	nd	nd

[a]Units are in 10^9 moles yr^{-1}. The aerosol equilibrium reaction budgets of NH_3 have been indirectly deduced from the NO_3 sink terms and by assuming that the total of all NH_3 sinks equals the emission. All source terms are marked in parentheses. Subscripts aq and ae indicate aqueous and aerosol phase respectively. "nd" means that the budget has not been determined (see Table 1) and "na" means that it is not defined and therefore not available for the particular component.

contribute significantly to the total AOD (see Discussion). Studies in the Netherlands in the 1980s and 1990s, for instance, showed that the contributions of sulfates and nitrates to aerosol scattering are comparable. Large parts of the fine particle mass could not be identified, and were presumed to be carbonaceous material. *Ten Brink et al.* [1996] speculated that the contribution of sulfate to particle scattering was between 30 and 40%. *Diederen et al.* [1985] found that sulfate scattering contributed 38% to the total aerosol extinction. These fractions which pertain to the Netherlands may be significantly different elsewhere. A complication is that the optical properties of especially organic aerosols are not well known. We therefore ignore this unknown aerosol fraction from the calculation of the AOD and focus on spatial patterns in the AOD field.

Following the approach of *Kiehl and Briegleb* [1993], the AOD is expressed as

$$AOD(\lambda) = f(RH, \lambda)\alpha(\lambda)B, \qquad (1)$$

where α is the mass extinction efficiency; i.e., extinction coefficient per unit of aerosol mass at relative humidity (RH) < 40%; B is the aerosol column burden; and $f(RH,\lambda)$ is the relative increase of the scattering coefficient at given RH to the scattering at low (<40%) RH. In equation (1), α and $f(RH)$ depend on the aerosol size distribution and chemical composition of the particles.

Following the above approach, the AOD of sulfate/nitrate aerosol at low RH is calculated from the model-predicted sulfate, nitrate, and ammonium column mass (B) using the mass extinction efficiency for ammonium-sulfate at 0.555μm. This implies that for nitrate aerosol the same size distribution is assumed as for sulfate aerosol.

The aerosol size distribution was assumed to be log-normal, with a geometric mean radius of 0.05 μm and a geometric standard deviation of 2.0. The dry density of the particles was taken as 1.7 g cm^{-3}. α was evaluated using a Mie code, and estimated to be 5 m^2 g^{-1} at 40% relative humidity and λ=0.555μm. This is in agreement with the values used in other studies [e.g., *Koch et al.*, 1999]. To account for the increase of aerosol extinction with increasing RH, the factor $f(RH,\lambda)$ is used in equation (1). This factor is the ratio between aerosol extinction at given RH to aerosol extinction at low RH (<40%). The increase of the scattering coefficient with increasing RH can be measured by humidity controlled nephelometry. *Veefkind et al.* [1996] have measured $f(RH)$ in the Netherlands in November 1993 for days characterized by continental air masses which are comparable with the situation under study August 1997. A polynomial fit to these experimental data is used to describe $f(RH)$. Mie calculations showed that the wavelength dependence of $f(RH)$ can be ignored. To compute the humidity effect on the AOD in TM3, the polynomial fit is used together with three-dimensional relative humidity fields which are calculated every 6 hours based on ECMWF temperature and specific humidity fields.

Figure 1 shows the monthly mean result of a global simulation of the AOD and the relative contribution of individual aerosol components for August 1997. It can be seen that the contribution of sulfate and water are the highest while the contribution of nitrate, at least for this NH summer month, is low.

4. ATSR-2 Dual View Retrieval

Data from ATSR-2 have been used to derive the spatial distribution of the aerosol optical depth (AOD) over Europe for August 1997 [*Robles-Gonzalez et al.*, 2000]. The ATSR-2 is a radiometer with seven wavelength bands, four of these bands are in the visible and near infrared (effective wavelengths 0.555, 0.659, 0.865, and 1.6 μm) and potentially useful for aerosol retrieval. A unique feature of the ATSR-2 is the dual-view capability providing two views of each region: first a forward view (zenith angle approximately 55°) and about 2 min later a nadir view. The AOD is retrieved in cloud-free areas using the dual-view algorithm developed by *Veefkind et al.* [1998]. This algorithm uses both the two-angle view and the spectral information of the ATSR-2 measurements to distinguish between atmospheric and surface contributions to the backscattered radiation. In contrast with most other existing aerosol retrieval methods the dual-view algorithm can in principle be used both over land and over the ocean. Over coastal waters, however, the algorithm still experiences some problems because of the complex determination of the angular dependence of the surface albedo when sediment is visible. Hence, in this work, we only focus on measurements over land. Once the atmospheric contribution is determined, the AOD is computed assuming a two-mode aerosol size distribution. The ratio between these modes is derived from the spectral behavior of the atmospheric radiance contribution.

The dual-view algorithm was validated by comparison with ground based sun photometer data for the east coast of the United States [*Veefkind et al.*, 1998] and for northwestern Europe [*Veefkind*, 1999]. These comparisons show that the satellite-retrieved AOD is well within 0.1 of the colocated Sun photometer data. This result yields confidence that the algorithm can be applied over most of western Europe, except possibly over highly reflecting surfaces, such as those covered with snow and semiarid areas.

5. Results

Previous work has been focused on the model's annual cycle, global budgets, and comparison of model results with monthly averaged measurements [e.g., *Jeuken*, 2000; *Barrie et al.*, 2001; *Lohmann et al.*, 2001; *Roelofs et al.*, 2001;]. In this paper we concentrate on shorter
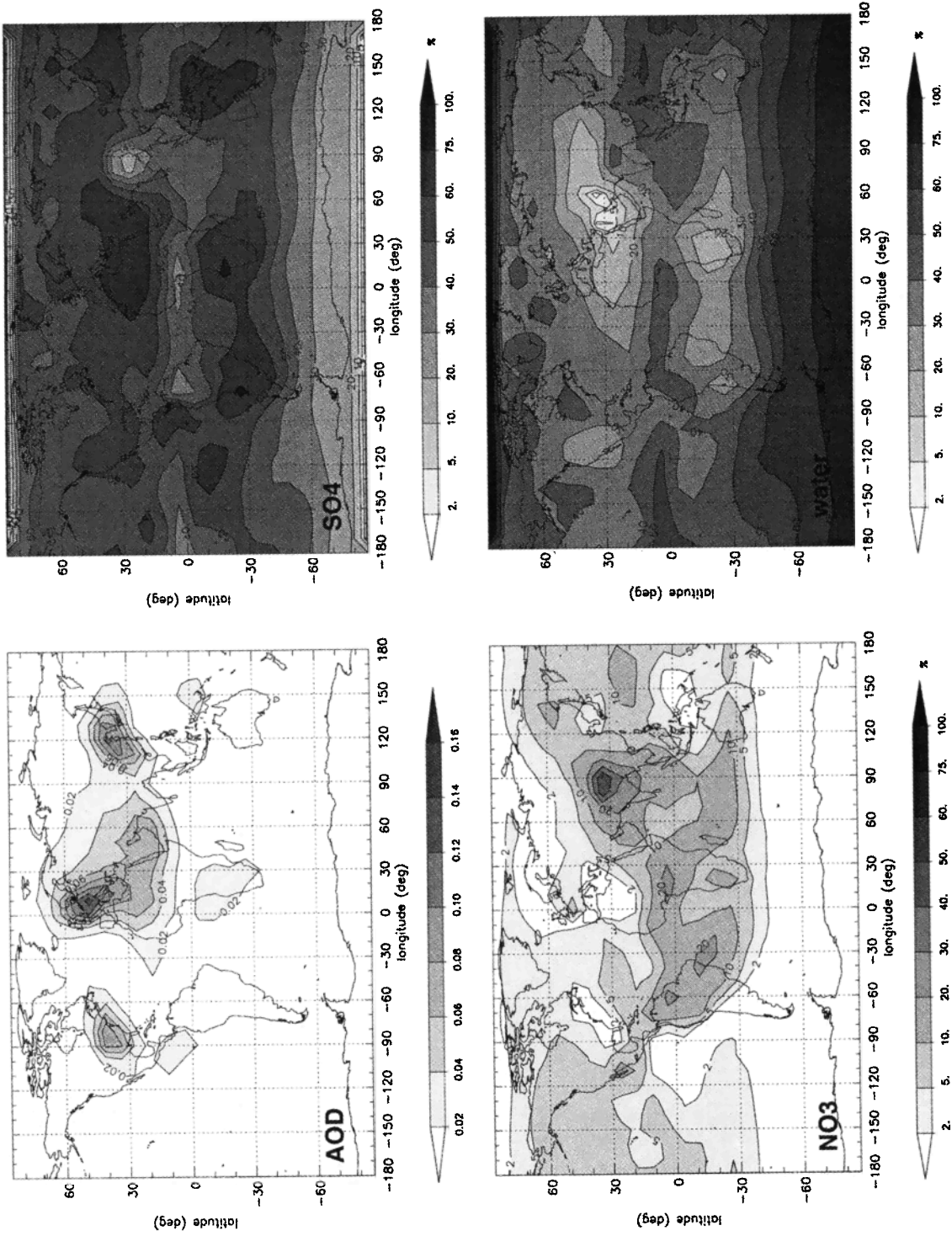
Figure 1. Monthly averaged AOD for August 1997 and the relative contributions of sulfate, nitrate, and water contained in aerosol. The latter is calculated by taking the difference between the AOD as calculated by equation (1) and the AOD calculated without taking into account hygroscopic growth ($f(RH)=1$).

timescales and on a specific summer episode, which is the month August 1997. This month is characterized by anomalous high temperatures and the presence of high-pressure systems over most of Europe. Also, precipitation has been lower than normal over central and northwestern Europe, while thunderstorms produce anomalously high precipitation over the south of France, Spain, and the Balkan [*Deutsche-Wetterdienst*, 1997]. As the ATSR-2 satellite instrument typically measures the same spot once every three days, we will focus on the ability of our model to simulate the day-to-day variability of aerosol concentrations. Besides comparing model results with the satellite AOD we also made a comparison of modeled surface concentrations with independent measurements from the European EMEP network [*EMEP*, 1998].

To be able to represent variability on timescales of a day or less, model simulations have been done at the, currently, highest possible resolution of TM3, which is 2.5° by 2.5° and 31 layers in the vertical. The model simulations were allowed one month spin-up time, by starting at July 1. It is investigated how well the TM3 model simulates observed surface aerosol concentrations for August 1997, the same month for which we have the ATSR-2 data available.

Because we know from experience with our model [*Jeuken*, 2000] that SO_2 concentrations are often too high, we also investigate the influence of emission reductions of SO_2. Therefore we define two model experiments: in experiment A5 the EDGAR emission data extrapolated to 1997 for SO_2 are replaced by the CORINAIR emission inventory for Europe and in experiment A4 the EDGAR data are used everywhere. As we know from section 2, the CORINAIR emissions are on average almost a factor of 2 lower than the European part of the EDGAR emissions since they are obtained by using more realistic emission factors. For August 1997, EDGAR emissions are about a factor 1.7 higher.

5.1. Comparison With Surface Measurements for August 1997

Model concentrations of SO_4^{2-}, NO_3^-, NH_4^+, NH_3, SO_2, and HNO_3 are stored every two hours at the locations of the measurement sites. About 200 sites from the EMEP network have been used. It must be noted that not all sites measured all species over the whole time period. Especially for NH_3 and particulate NO_3^- only a few measurements are available. In addition, measurements of nitrate are subject to considerable uncertainties [*Harrison and Kitto*, 1990]. Especially when filter packs without denuder system are used, losses due to evaporation of nitrate may be as large as 100% [*Pakkanen et al.*, 1999]. This is the case at most measurements sites.

Table 3 provides a short statistical overview of the comparison of both model simulations A4 and A5 with the daily average EMEP measurements for August 1997.

Table 3. Correlations and Average Differences Between Observation and the Model, Based on Daily Averages for All Available EMEP Stations for August 1997.

| | | Correlation | | Difference (O-M), $\mu g\ m^{-3}$ | |
	N	A4	A5	A4	A5
SO_2	1868	0.36	0.39	-4.2 ± 5.4	-2.7 ± 4.3
SO_4^{2-}	2059	0.56	0.58	-0.3 ± 1.8	0.0 ± 0.8
NH_x	956	0.66	0.66	-0.5 ± 1.7	-0.40 ± 1.7
XNO_3	884	0.60	0.61	-0.5 ± 0.9	-0.5 ± 0.9
NO_3	401	0.66	0.66	0.3 ± 0.3	0.3 ± 0.3

XNO_3 is the sum of NO_3^- and HNO_3 and NH_x of NH_3 and NH_4^+. N is the total number of daily measurements (number of stations times number of days).

Aerosol surface concentrations are well simulated by the model. Especially for sulfate the average differences are small. A relatively high correlation is found for total NH_x. SO_2 is strongly overestimated by the model, even when the CORINAIR emissions are applied. Using the CORINAIR emissions leads to better agreement between model and measurements for SO_2, sulfate and to a lesser extent total NH_x.

Figures 2-4 show simulated and observed aerosol concentrations for a small selection of EMEP sites. Sites were selected such that the whole European domain is more or less covered. It is again shown (Figure 2) that the agreement between model and observations is good for sulfate as both model runs A4 and A5 simulate the day-to-day variability as well as the absolute magnitude of the concentrations well. Even at the sites where SO_2 (not shown) is overestimated by 100% (e.g., Langenbrugge, Tange) sulfate is within 10 to 20% of the observations. Best agreement is clearly obtained with simulation A5.

Results for particulate nitrate of 4 of the 12 available EMEP sites are shown in Figure 3. Nitrate is difficult to model since its formation strongly depends on humidity, temperature and the concentrations of sulfate and ammonia. If the ammonia concentrations do not exceed the sulfate concentrations, no nitrate can partition into the aerosol phase. For Ispra in Italy, Vreedepeel in the Netherlands, and Leba in Poland, model values are in reasonable agreement with the observations. At Liesek in Slowakia, which is a station at a higher altitude of almost 900 m, the model clearly underestimates the particulate nitrate concentration. This may indicate that the decrease of ammonia and hence nitrate concentration with altitude is too strong in the model. However, comparison with more higher altitude stations or with profile measurements should point this out. While particulate nitrate is on average too low, the sum of nitrate plus nitric acid is too high compared to the observations at the 8 sites that measure the sum of these compo-
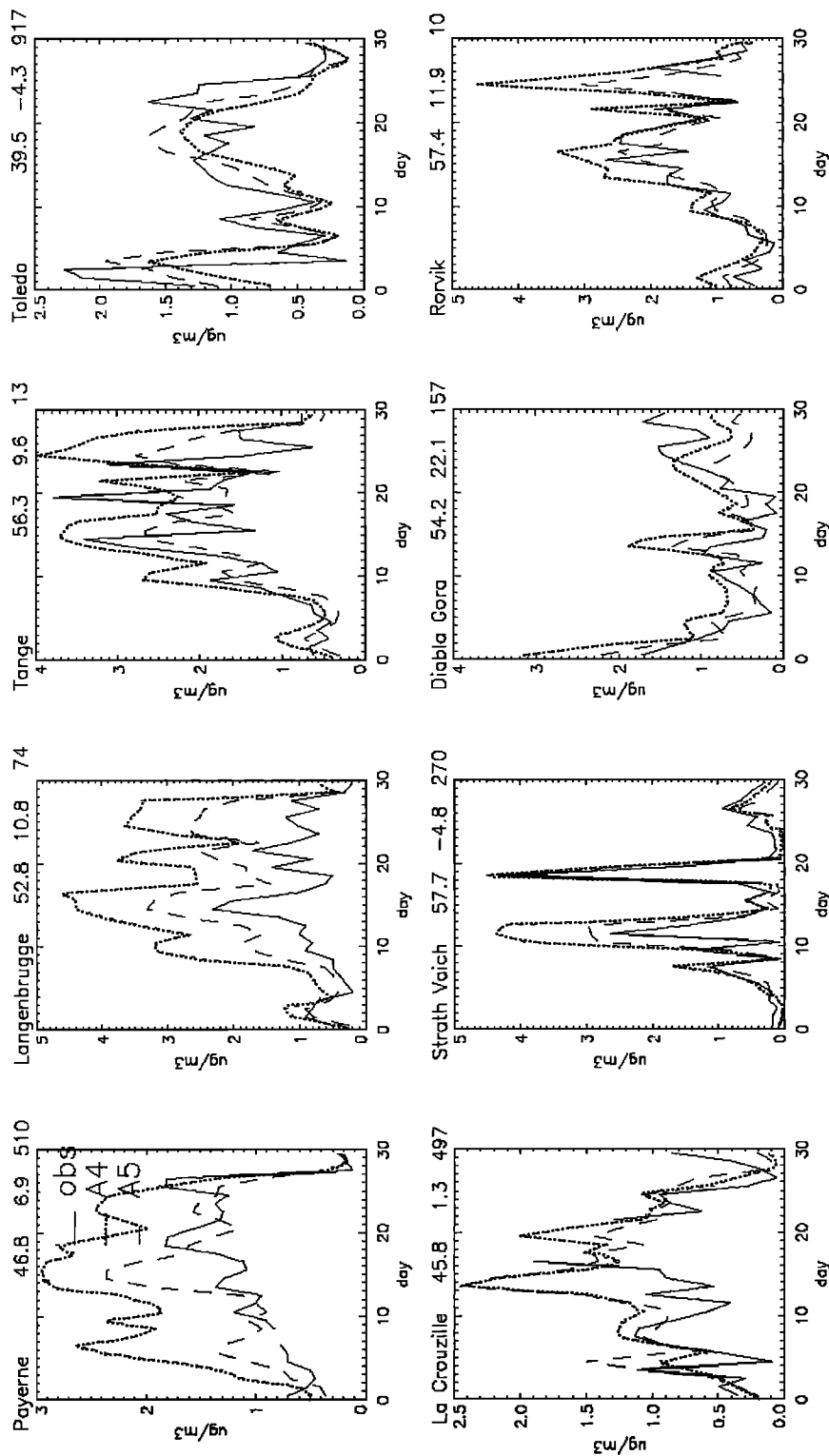
Figure 2. Comparison of daily averaged model values and measurements of SO_4^{2-} for selected EMEP sites (August 1997). Numbers in the headers indicate latitude, longitude, and height of the station, respectively.
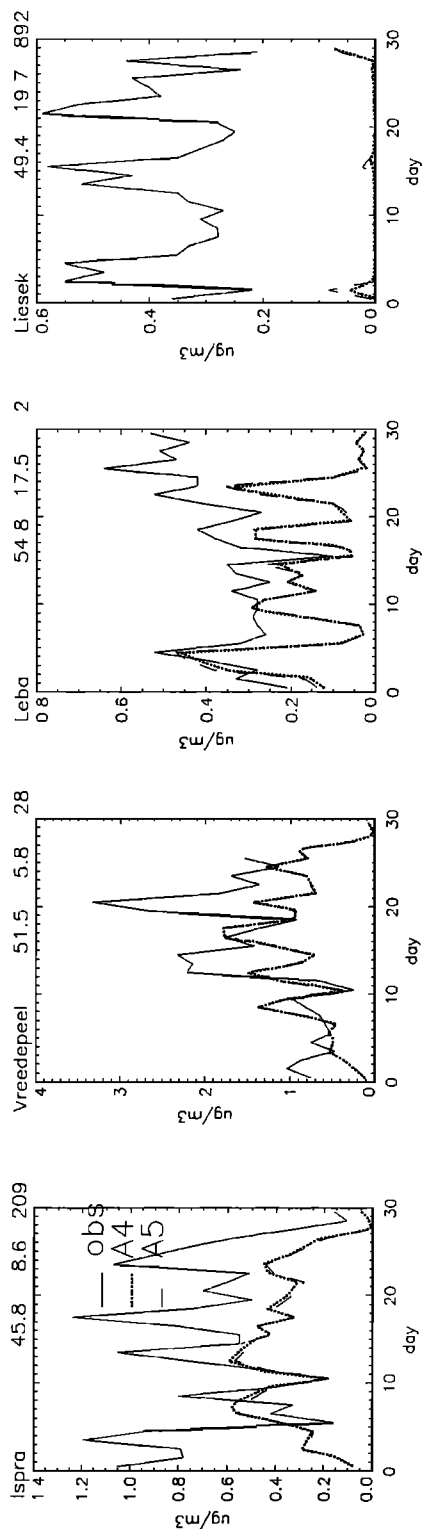
Figure 3. Comparison of daily averaged model values and measurements of NO_3^- for selected EMEP sites (August 1997)
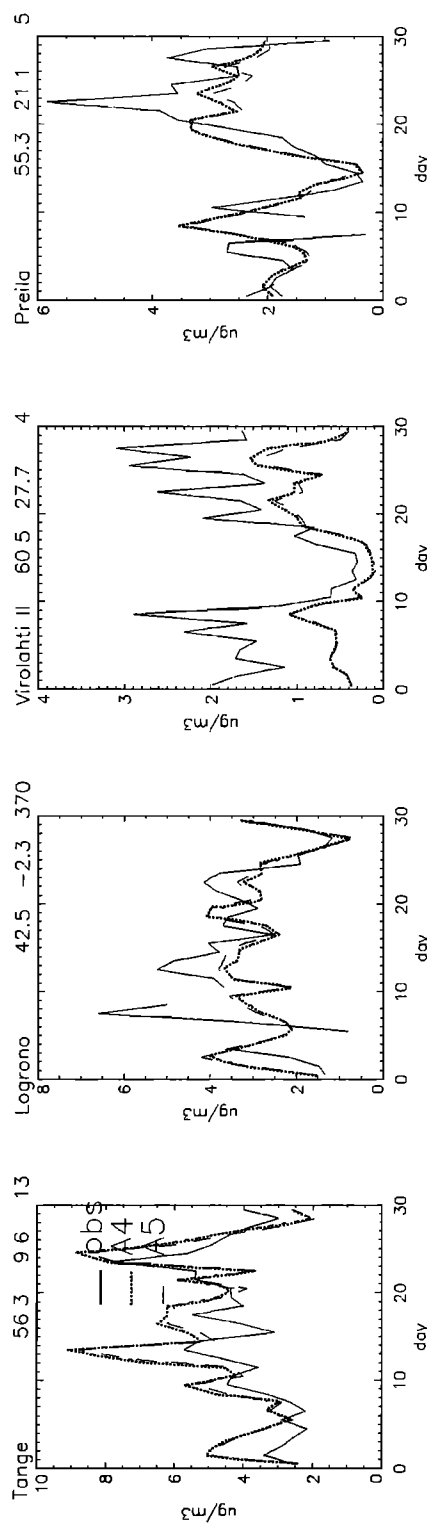

Figure 4. Comparison of daily averaged model values and measurements of $NH_4^+ + NH_3$ for selected EMEP sites (August 1997).

nents. This indicates that the availability of HNO_3 is not limiting the formation of nitrate aerosol.

The sum of ammonium and ammonia is measured at about 24 sites. In most cases ammonium concentrations are strongly correlated with sulfate (e.g., Tange, Denmark). As was the case for sulfate, agreement between model and observations is quite good (see also Table). Ammonia is a difficult species to model due to its short lifetime and heterogeneous sources. However, based on this result, there seems to be no reason to doubt about the quality of the NH_3 emissions in TM3 at least for Europe [Bouwman et al., 1997]. In the model for this particular month the fraction ammonia in NH_x is on average 50% over the European continent at surface level. Colocated ammonia measurements would, however, be needed to find out about the fraction ammonia in measured NH_x. It is important to model this fraction correctly, since the pH of cloud water and therefore the cloud reaction rates strongly depend on the concentrations of NH_4^+. In addition, long-range transport of ammonium can contribute significantly to acid deposition at remote locations.

5.2. Comparison With AOD Retrieved From ATSR-2

We compare the AOD of the TM3 aerosol field with the AOD of ATSR-2 at $0.555\mu m$. For this purpose, all available cloud-free ATSR-2 pixels for August 1997 are combined into a monthly averaged composite field for Europe. For each overpass the satellite pixels with a resolution of 0.1° by 0.1° are gathered within a model grid cell of 2.5° by 2.5°. Only if more than 100 (±15% of possible coverage) valid pixels are encountered the median value is taken as the satellite-retrieved AOD for that particular grid cell. Otherwise the grid cell for that day is marked invalid. Such a selection is made in order to find a compromise between representativity of the resulting grid cell average or median and the amount of data left. The upper panels of Plate 1 show the number of valid overpasses obtained in the above described manner for the month August 1997 and the monthly average composite field derived from these overpasses. Such a composite field presents a rather biased view of the monthly averaged aerosol field. For instance, over England and Scotland the average consist of a few points in time only, while for other more sunny areas each overpass might be included. In addition, the high values of the ATSR-2 composite field (Plate 1, upper right panel) probably present an upper limit for the aerosol pollution over Europe, since clear-sky weather situations over especially western Europe are usually associated with easterly flows over major source regions and associated with little precipitation scavenging.

In this section again we focus on the two model simulations, A4 and A5. It is investigated whether the change in the input emissions is visible in the simulated AOD patterns, where the emissions in A4 are probably too high. Model output was generated at 11 UTC, the approximate time of overpass for ATSR-2 over Europe. The composite average is calculated for the valid ATSR-2 pixels, as described above. The results are shown in the two middle panels of Plate 1. The two lower panels show the true monthly averages of the model simulations. As expected the monthly averaged AOD is somewhat lower than the composite average since it is not biased towards cloud-free wetter situations. However, the main pattern is very similar.

Plate 1 shows that model captures the main features observed by ATSR-2, like the maxima over the Po valley and the south of Italy, the Barcelona area, the maximum over the Netherlands, and the urban areas along the Scandinavian coast. Noteworthy are the well-simulated peak values over England, as they are an average of one or two overpasses only. Also, the low AOD values over north Scandinavia are simulated well.

However, also some important sources of aerosols seem to be missing, especially over southern France, Spain, eastern Europe, and the Balkan. However, as indicated earlier, these regions were also exposed to extreme weather conditions, perhaps leading to a too effective wet removal of aerosol and precursor.

Model simulation A5 in general is not much different from A4. The AOD pattern over Spain seems to be slightly better simulated when using the CORINAIR emissions for SO_2. Also, the maximum over the Netherlands is less pronounced, which is in better agreement with ATSR-2.

A more quantitative comparison between the satellite data and model simulation is shown in Table 4. Correlations and average differences for all the valid 2.5° by 2.5° pixels have been calculated. In addition, this calculation has been done separately for different areas. The correlation between observations an model simulation is with 0.68 quite good. The best correlation is obtained over northwest and eastern Europe. The worst correlation we find over southeast Europe. The absolute difference in AOD is smallest over Scandinavia and largest over East and South-East Europe.

On average there is a difference between the model simulations and ATSR-2 in the AOD of 0.17 and 0.19 for model simulation A4 and A5, respectively. This difference is fairly constant over Europe, with the exception of Scandinavia where it is about 0.05 lower. We should not forget that the TM3 model with its coarse resolution only simulates the water soluble aerosol species SO_4 and NO_3 and the complex mix of various other aerosol species is not included. Desert dust can have an important influence over the south of Europe [Guelle et al., 2001]. Organic aerosols can have an important contribution to the AOD over the whole of Europe [Kanakidou et al., 2000]. ATSR-2 does observe the whole aerosol burden.

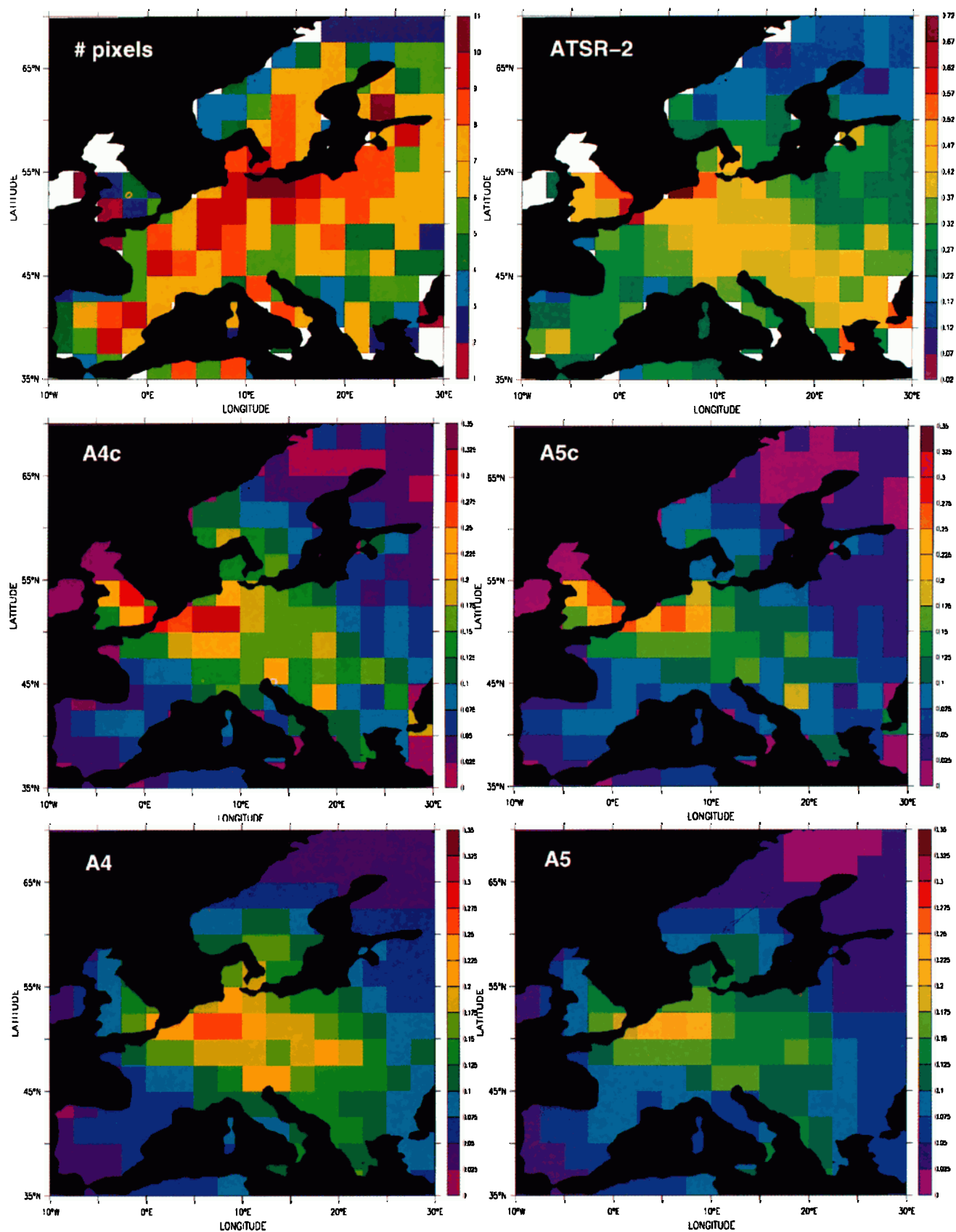In contrast with the results of the previous section, model simulation A4 agrees somewhat better with the

Plate 1. Composite monthly averaged field of the AOD at 555 μm for Europe August 1997. Only data for cloud-free pixels have been used. (top left) Number of overpasses per grid cell, (top right) ATSR-2, (middle left and right) TM3 model simulations A4 and A5 respectively, including a satellite retrieval consistent sampling procedure. (bottom left and right) True monthly mean model fields. Note the the difference in scale between the satellite retrieval and the model field.

Table 4. Correlations and Average Differences between the AOD from ATSR-2 and from the Model, for Different Regions and Model Simulations A4 and A5.

	N	Correlation		Difference (O-M)	
		A4	A5	A4	A5
Europe (35°N-70°N,10°W-30°E)	811	0.68	0.66	0.17	0.19
NW Europe (50°N-70°N,10°W-12.5°E)	121	0.74	0.71	0.15	0.19
SW Europe (35°N-50°N,10°W-10°E)	211	0.63	0.61	0.18	0.18
SE Europe (35°N-45°N,10°E-30°E)	82	0.44	0.40	0.24	0.26
E Europe (45°N-55°N,12.5°E-30°E)	180	0.70	0.69	0.20	0.24
Scandinavia (55° N-70°N,5°E-30°E)	255	0.63	0.59	0.12	0.14

observations than simulation A5. In the next paragraph this issue will be further discussed.

6. Discussion and Conclusions

In this paper two main subjects have been studied. First, the concentrations of various aerosol components from two model simulations with each a different emission scenario for SO_2 have been compared to surface measurements. Second, AOD has been computed from the simulated aerosol masses and compared to the AOD as retrieved from ATSR-2 measurements.

We have seen that surface concentrations of the aerosol components sulfate and ammonium and to a somewhat lesser extent nitrate are well simulated by the model for the episode discussed in this paper. There is almost a factor of 2 reduction in SO_2 surface concentrations over Europe when using the CORINAIR emissions which brings SO_2 concentrations in better agreement with measurements. However, similar as in many other models [Barrie et al., 2001; Chin et al., 1996], surface concentrations of SO_2 are still strongly overestimated by the model over large parts of Europe [see also Jeuken, 2000]. Also, sulfate surface concentrations are in bet-

ter agreement with the measurements when using the CORINAIR emissions. In contrast with SO_2 there is no systematic difference with the observed concentrations.

Going from scenario A4 to A5 the factor of 2 reduction in SO_2 surface concentrations does not yield a similar reduction in sulfate in our model. The reduction in sulfate by only 30%, indicates that excess SO_2 is not necessarily converted to sulfate. These results for SO_2 and sulfate suggest that in case of higher SO_2 emissions, a relatively larger part of emitted SO_2 at surface level is removed before it is converted to sulfate. This is shown in Table 5, where for high emission scenario A4 a higher fraction of the emissions is removed by dry deposition. Table 5 also shows that the total column burden reduction of sulfate is 37% comparing A4 and A5, which is rather similar to the SO_2 emission reduction. This indicates that the nonlinearity between SO_2 emissions and sulfate formation near the surface is compensated by chemistry at higher altitudes. This reduction of sulfate predominantly occurs below 1000m, since the sulfate amounts above 1000 m are remarkably constant.

The budgets of other aerosol components (not shown) are sensitive to the SO_2 emissions although to a lesser extent than sulfate. For instance for scenario A5 the

Table 5. Boundary Layer, Free Tropospheric and Total Volume Budgets and Burden for SO_2 and Sulfate for the Area from 10°W to 50°E and 30°N to 85°N and the Month August 1997.

	Below 1000 m		Above 1000 m		Total	
	A4	A5	A4	A5	A4	A5
Net SO_2 input (Tg)	1.30	0.81	0.31	0.20	1.61	1.01
Dry deposition, %	46	40	0	0	37	33
Wet deposition, %	22	33	22	25	22	32
Gas phase oxidation, %	10	6	13	15	14	6
In-cloud oxidation, %	22	21	65	60	30	29
SO_2 burden, 10^6 kg	32.0	16.0	14.5	9.5	46.5	25.5
Sulfate burden, 10^6 kg	30.0	18.0	28.5	19.0	58.5	37

Percentages indicate the amount of the SO_2 input in the domain is converted or removed. The net SO_2 input is calculated by adding the emissions and the net inflow from outside the domain.

aerosol is more neutralized by ammonium than for scenario A4. This partly explains why the average differences in AOD between A4 and A5 is less than 37%. In addition, the AOD is for a large part determined by the hygroscopic growth of the aerosol. Near the surface, where the differences in sulfate between the two scenarios is smallest, this growth is most significant.

About 40 to 50 % of the measured AOD can be explained by the model simulations. At least, other aerosol components need to be included in the model to reduce the difference between observed and simulated AOD. Nevertheless, the correlations between model and measurements are quite good. This correlation includes both the covariance in time and space between model and observations. Two main conclusions can be drawn from this result. First of all, it indicates that the model is well able to simulate the order of magnitude, location and timing of important aerosol sources and sinks and the growth of aerosols due to water uptake. Second, there should be a good correlation between the simulated and missing aerosol species. This sounds only plausible if this missing aerosol is like sulfate related to anthropogenic activity. This is the case for part of the organic aerosol. The enhancement of organic aerosol formation in the polluted boundary layer [Griffin et al., 1999; Kanakidou et al., 2000] also takes place under anthropogenically influenced atmospheric conditions. In southern Europe, where the discrepancy between model and observations is largest and the correlation lowest, desert dust either locally produced or transported from the Sahara dessert could play a role. On the basis of results obtained by Guelle et al. [2000], we do not expect that the contribution of sea-salt to the AOD is larger than 10% over the continental regions of Europe.

Besides that we do not account for all aerosol components in the model, there are possible problems with the modeling of the vertical distribution of sulfate, nitrate, and ammonium. We have seen that surface aerosol concentrations are well simulated by the model. This result might be representative for the concentrations in the boundary layer. However, measurements [e.g., Lohmann et al., 2001] and model results (e.g., Table 1) indicate that half of the aerosol burden is above the boundary layer. This could either indicate that removal of aerosols by precipitation is too effective or that not enough SO_2 is oxidized to form sulfate. Other authors have suggested that an additional oxidation mechanism for SO_2 would be needed to explain the discrepancy between modeled and observed SO_2 and sulfate concentrations [e.g., Kasibhatla et al., 1997]. In addition, it was suggested [e.g., Dentener et al., 1999; Jeuken, 2000] that vertical mixing in the boundary layer in TM3 is insufficient. Increased vertical transport of SO_2 to the clouds and increased mixing of free tropospheric air, containing oxidants for SO_2, and boundary layer air will lead to an increase of the sulfate burden above the surface. This mechanism would both decrease the too high SO_2 surface concentrations and increase the

total aerosol column. To really be able to verify these hypotheses, concurrent profile measurements of aerosol components, precursors, and oxidants are needed.

Whereas for the surface concentrations the model simulation with the CORINAIR emissions clearly gives the best results, this is not the case for total aerosol column. Given the uncertainty in the modeling of the total aerosol column, this is not surprising. However, it also makes clear that the use of the satellite-retrieved total AOD for validating model changes remains limited as long as the model does not simulate the AOD of all relevant aerosol components.

Uncertainties in the estimates of the optical parameters in both the model as well as the retrieval algorithm may account for large uncertainties as well. The total uncertainty in the satellite retrieval was quantified by comparison with sun photometer measurements and estimated to be within 0.1 in AOD [Veefkind et al., 1998]. The extinction efficiency α is strongly dependent on the size distribution of the aerosol population. Within the size range between 0.1 and 1 μm, where most sulfate and nitrate is in, α varies from 2 until 10 m^2 g^{-1} for a wavelength of 0.53μm [Schwartz, 1996] and is therefore strongly dependent on the chosen size distribution. To gain accuracy for α the size distribution of aerosols should be explicitly modeled. In addition, the increase of light scattering with increasing humidity f(RH) is dependent on the chemical composition of the aerosol. However, for the simulations done in this paper we have used a function based on measurements of aerosol samples in the Netherlands. Since the aerosol composition varies spatially, errors are introduced by applying this function everywhere. The aerosol equilibrium model used in our model explicitly calculates the water uptake of aerosol depending on its chemical composition [Metzger, 2000]. In the future this information should be used to estimate the dependence of the scattering coefficient on the relative humidity.

So the challenge remains to match the AOD, which is a bulk optical quantity, with model-calculated masses of a limited number of aerosol components. In this paper we have calculated the AOD from the modeled aerosol mass using a simplified optical model. For this optical model the parameters have been estimated as good as possible using generally accepted assumptions about the properties of ammonium-nitrate and sulfate aerosol as well as observations of hygroscopic growth. In addition, available four dimensional information like the relative humidity field and aerosol mass field have been maximally used, i.e., calculate the AOD on-line per grid cell and time step before columns are integrated.

Were we 100% certain about our calculations and the AOD retrieval from ATSR, we would be able to estimate the contribution of missing aerosol species. However, as indicated before, we know that there are many uncertainties. The comparison of modeled concentrations with surface measurement has shown that the uncertainty for (surface) sulfate is relatively low and for

nitrate is still quite high. The model tends to underestimate nitrate. The fact that SO_2 is overestimated by the model and remains unoxidized and the experience that vertical mixing is underestimated while scavenging maybe too effective [*Jeuken*, 2000] lead us to believe that the sulfate column burden is underestimated [*Jeuken*, 2000].

Because the average observed AOD is more than a factor of 2 larger than the average simulated AOD, we might, despite all uncertainties, conclude that there must be a considerable contribution of the missing aerosol species, most likely organic aerosol and mineral aerosol. We can give only a very tentative quantitative indication of this contribution, based upon before mentioned arguments and based upon an average simulated AOD of 0.1 (A4) and observed AOD of 0.27. If we assume that averaged over the whole period and domain the uncertainty in the optical parameters is 25% , that we underestimate the sulfate column by 25% and the nitrate column by 50% and that the observational uncertainty is on average 0.05 in AOD, the AOD of the missing aerosol components is estimated as 0.14 ± 0.06. This contribution is of the same order as the contribution of sulfate plus nitrate.

More and more detailed observations are very much needed to quantify uncertainties. For our study, simultaneous measurements of the organic and mineral aerosol fraction would have been of great help. Measured concentration profiles of aerosol components would be helpful to evaluate the model performance away from the surface. Measurements of the aerosol size distributions at more than one location and altitude would be needed to evaluate part of the assumptions used in the Mie calculations. Cloud chamber experiments at other locations than Petten would be needed to evaluate the validity of f(RH). Such detailed measurements can only be obtained from measurement campaigns, such as ACE 2. For model evaluation the measurements should preferably be applicable to the period under study and for the sake of reproducibility cover more than one location. Campaigns can comply with the first demand but not with the second. Unfortunately, the ACE 2 area is situated just outside our study area. In the near future a zoom version of the model will become available, which will be specifically used for comparison with measurements from campaigns.

Acknowledgments

References

Adams, P. J., J. H. Seinfeld, and D. M. Koch, Global concentrations of tropospheric sulfate, nitrate, and ammonium aerosol simulated in a general circulation model, *J. Geophys. Res.*, *104*, 13,791–13,823, 1999.

Andres, R. J., and A. D. Kasgnoc, A time-averaged inventory of aerial volcanic sulfur emissions, *J. Geophys. Res.*, *103*, 25,251–25,261, 1998.

Balkanski, Y. J., D. J. Jacob, G. M. Gardner, W. C. Graustein, and K. K. Turekian, Transport and residence times of tropospheric aerosols inferred from a global three-dimensional simulation of ^{210}Pb, *J. Geophys. Res.*, *98*, 20,573–20,586, 1993.

Barrie, L. A., et al., A comparison of large scale atmospheric sulphate aerosol models COSAM): overview and highlights., *Tellus B, in press*, 2001.

Beljaars, A. C. M., and P. Viterbo, Role of the boundary layer in a numerical weather prediction model, in *Clear and Cloudy Boundary Layers*, edited by A. A. M. Holtslag and P. G. Duynkerke, pp. 85–110, KNAW, Amsterdam, The Netherlands, 1998.

Benkovitz, C. M., M. T. Scholtz, J. Pacyna, L. Tarrason, J. Dignon, E. C. Voldner, P. A. Spiro, J. A. Logan, and T. E. Graedel, Global gridded inventories of anthropogenic emissions of sulfur and nitrogen, *J. Geophys. Res.*, *101*, 29,239–29,253, 1996.

Bouwman, A. F., D. S. Lee, W. A. H. Asman, F. J. Dentener, K. W. V. D. Hoek, and J. G. J. Olivier, A global high-resolution emission inventory for ammonia, *Global Biogeochem. Cycles*, *11*, 561–587, 1997.

Charlson, R. J., S. E. Schwartz, J. M. Hales, R. D. Cess, J. A. J. Coackley, J. E. Hansen, and D. J. Hofmann, Climate forcing by anthropogenic aerosols, *Science, 255*, 423–430, 1992.

Chin, M., D. J. Jacob, G. M. Gardner, M. S. Foreman-Fowler, and P. A. Spiro, A global three-dimensional model of tropospheric sulfate, *J. Geophys. Res.*, *101*, 22,869–22,889, 1996.

Chuang, C. C., and J. E. Penner, Effects of anthropogenic sulfate on cloud droplet nucleation and optical properties, *Tellus, 47*, 566–577, 1995.

Claussen, M., U. Lohmann, E. Roecknet, and U. Shulzweida, A global data set of land-surface parameters, *Tech. Rep. 135*, Max Planck Inst. für Meteorol., Hamburg, Germany, 1994.

Cooke, W. F., and J. J. N. Wilson, A global black carbon aerosol model, *J. Geophys. Res.*, *101*, 19,395–19,409, 1996.

Dana, M. T., and J. M. Hales, Statistical aspects of the washout of polydisperse aerosols, *Atmos. Environ.*, *10*, 45–50, 1991.

Dentener, F., and P. J. Crutzen, Reaction of N_2O_5 on tropospheric aerosols: Impact on the global distributions of NO_x, O_3, and OH, *J. Geophys. Res.*, *98*, 7149–7163, 1993.

Dentener, F., and P. J. Crutzen, A global 3D model of the ammonia cycle, *J. Atmos. Chem.*, *19*, 331–369, 1994.

Dentener, F., J. Feichter, and A. Jeuken, Simulation of the transport of Radon^{222} using on-line and off-line global models at different horizontal resolutions: A detailed comparison with measurements, *Tellus, Ser. B 51*, 573–602, 1999.

Deutsche-Wetterdienst, Review August 1997, *Tech. Rep.*, Deutsche Wetterdienst, Offenbach, Germany, 1997.

Diederen, H., R. Guicherit, and J. Hollander, Visibility reduction by air pollution in the Netherlands, *Atmos. Environ.*, *19*, 377–383, 1985.

European Monitoring and Evaluation Programme, Transboundary acidifying air pollution in Europe, in *MSC-W Status Report 1998 - Part 1*, 48 pp., Meteorol. Syn. Cent.-West, Norw. Meteorol. Inst., Oslo, Norway, 1998.

Feichter, J., E. Kjellström, H. Rodhe, F. Dentener, J. Lelieveld, and G.-J. Roelofs, Simulation of the tropospheric sulfur cycle in a global climate model, *Atmos. Environ.*, *30*, 1693–1707, 1996.

Ganzeveld, L., J. Lelieveld, and G.-J. Roelofs, Dry deposition parametrization of sulfur oxides in a chemistry and general circulation model, *J. Geophys. Res.*, *103*, 5679–5694, 1998.

Gery, M. W., G. Z. Whitten, J. P. Killus, and M. Dodge, A photochemical kinetics mechanism for urban and regional scale computer modeling, *J. Geophys. Res.*, *94*, 925–956, 1989.

Gong, S. L., L. A. Barrie, J. Prospero, D. L. Savoie, G. P. Ayers, J.-P. Blanchet, and L. Spacek, Modeling sea-salt aerosol in the atmosphere, 2, Atmospheric concentrations and fluxes, *J. Geophys. Res.*, *102*, 3819–3830, 1997.

Griffin, R. J., D. R. Cocker, R. C. Flagan, and J. H. Seinfeld, Organic aerosol formation from the oxidation of biogenic hydrocarbons, *J. Geophys. Res.*, *104*, 3555–3567, 1999.

Guelle, W., Y. J. Balkanski, J. E. Dibb, M. Schulz, and F. Dulac, Wet deposition in a global size-dependent areosol transport model, 1, Comparison of a 1 year ^{210}Pb simulation with ground measuremens, *J. Geophys. Res.*, *103*, 11,429–11,445, 1998a.

Guelle, W., Y. J. Balkanski, J. E. Dibb, M. Schulz, and F. Dulac, Wet deposition in a global size-dependent areosol transport model; 2, Influence of the scavenging scheme on ^{210}Pb vertical profiles, surface concentrations, and deposition, *J. Geophys. Res.*, *103*, 28,875–28,891, 1998b.

Guelle, W., Y. J. Balkanski, M. Schulz, B. Marticorena, G. Bergametti, C. Moulin, R. Arimoto, and K. D. Perry, Modeling the atmospheric distribution of mineral aerosol: Comparison with ground measurements and satellite observations for yearly and synoptic timescales over the North Atlantic, *J. Geophys. Res.*, *105*, 1997-2012, 2000.

Guelle, W., Y. Balkanski, M. Schulz, and F. Dentener, Influence of the source formulation on modeling the atmospheric global distribution of sea-salt aerosol, *J. Geophys. Res.*, in press, 2001.

Harrison, M. R., and A. M. N. Kitto, Filed intercomparison of filter pack and denuder sampling methods for reactive gaseous and particulate pollutants, *Atmos. Environ., Part A*, *24*, 2633–2640, 1990.

Haywood, J. M., V. Ramaswamy, and B. Soden, Tropospheric aerosol climate forcing in clear-sky satellite observations over the oceans, *Science*, *283*, 1299–1303, 1997.

Heimann, M., The global atmospheric tracer model tm2, *Tech. Rep. 10*, Dtsch. Klima Rechenzentrum, Modell., Hamburg, Germany, 1995.

Holtslag, A. A. M., and B. A. Boville, Local versus nonlocal boundary-layer diffusion in a global climate model, *J. Clim.*, *6*, 1825–1842, 1993.

Houweling, S., F. Dentener, and J. Lelieveld, The impact of nonmethane hydrocarbon compounds on tropospheric chemistry, *J. Geophys. Res.*, *103*, 10,673-10,696, 1998.

Jaenicke, R. *Landolt-Börnstein Zhalenwerte und Funktionen aus Naturwissenshaften und Technik, Vol 4, Meteorologie, Teilband B: Physikalische und chemische Eigenschaften der Luft*, pp. 391-457, Springer-Verlag, New York, 1988.

Jeuken, A., Evaluation of chemistry and climate models using measurements and data assimilation, Ph.D. thesis, University of Technology Eindhoven, The Netherlands, 2000. (Available at http://alexandria.tue.nl-/extra2/200001283.pdf.)

Kanakidou, M., K. Tsigaridis, F. Dentener, and P. Crutzen, Human-activity-enhanced formation of organic aerosols by biogenic hydrocarbon oxidation., *J. Geophys. Res.*, 105, 9243-9254, 2000.

Kasibhatla, P., W. L. Chameides, and J. S. John, A three-dimensional global model investigation of seasonal variations in the atmospheric burden of anthropogenic sulfate aerosols, *J. Geophys. Res.*, *102*, 3737–3759, 1997.

Kettle, A. J., et al., A global database of sea surface dimethylsulfide (DMS) measurements and a procedure to predict sea surface DMS as a function of latitude, longitude, and month, *Global Biogeochem. Cycles*, *13*, 399–444, 1999.

Kiehl, J. T., and B. P. Briegleb, The relative roles of sulfate aerosols and greenhouse gases in climate forcing, *Science*, *260*, 311–314, 1993.

Koch, D., D. Jacob, I. Tegen, D. Rind, and M. Chin, Tropospheric sulfur simulation and sulfate direct radiative forcing in the Goddard Institute for Space Studies GCM., *J. Geophys. Res.*, *104*, 23,799–23,822, 1999.

Krol, M., and M. van Weele, Implication of variation of photodissociation rates for global atmospheric chemistry, *Atmos. Environ.*, *31*, 1257–1273, 1997.

Langner, J., and H. Rodhe, A global three-dimensional model of the tropospheric sulfur cycle, *J. Atmos. Chem.*, *13*, 225–263, 1991.

Lelieveld, J., and F. Dentener, What controls tropospheric ozone?, *J. Geophys. Res.*, *105*, 3531-3551, 2000.

Liousse, C., J. E. Pennner, C. Chuang, J. J. Walton, H. Eddleman, and H. Cachier, A global three-dimensional model study of carbonaceous aerosols, *J. Geophys. Res.*, *101*, 19,411–19,432, 1996.

Liss, P., and L. Merlivat, Air-sea gas exchange rates: Introduction and synthesis, in *The Role of Sea-Air Exchange in Geochemical Cycling*, edited by P. Menard, pp. 113–127, D. Reidel, Norwell, Mass., 1986.

Lohmann, U., et al., Comparison of the vertical distribution of sulfur species from models participated in the COSAM exercise with observations, *J. Geophys. Res.*, in press, 2001.

Louis, J. F., M. Tiedtke, and J. F. Geleyn, A short history of PBL parameterization at ECMWF, in *Proceedings of the ECMWF Workshop on Boundary-Layer Parameterization*, pp. 59–79, Eur. Cent. for Medium-Range Weather Forecasts, Reading, England, 1982.

Metzger, S., Gas/aerosol partioning: A simplified method for global modeling, Ph.D. thesis, Utrecht, The Netherlands, 2000. (Available at http://pablo.ubu.ruu.nl/ proef-sch/fysst.html).

Metzger, S., F. Dentener, and J. Lelieveld, Aerosol multiphase chemistry - a parameterization for global modeling, *Internal Rep. 99-12*, Inst. for Mar. and Atmos. Res. Utrecht, Utrecht, The Netherlands, 1999.

Nenes, A., C. Pilinis, and S. N. Pandis, Isorropia: A new thermodynamic model for multiphase multicomponent inorganic aerosols, *Aquat. Geochem.*, *4*, 123–152, 1998.

Olivier, J., Description of EDGAR version 2.0, *Tech. Rep. 771060002*, Natl. Inst. of Public Health and the Environ., Bilthoven, The Netherlands, 1996.

Olson, J., J. A. Watts, and L. J. Allison, Carbon inlive vegetation of major world ecosystems, *Tech. Rep. ORNL-5862*, Oak Ridge Natl. Lab., Oak Ridge, Tenn., 1983.

Pakkanen, T. A., et al., Nordic intercomparison for measurements of major atmospheric nitrogen species, *J. Aerosol Sci.*, *30*, 247–263, 1999.

Pham, M., J.-F. Müller, G. P. Brasseur, C. Granier, and G. Mégie, A three-dimensional study of the tropospheric sulfur cycle, *J. Geophys. Res.*, *100*, 26,061–26,092, 1995.

Robles-Gonzalez, C., J. P. Veefkind, and G. de Leeuw, Aerosol optical depth over Europe in august 1997, *Geophys. Res. Let.*, *Vol. 27. No. 7*, 955-958, 2000.

Roelofs, G.-J., and J. Lelieveld, Distribution and budget of O_3 in the troposphere calculated with a chemistry general circulation model, *J. Geophys. Res.*, *100*, 20,983–20,998, 1995.

Roelofs, G.-J., J. Lelieveld, and L. Ganzeveld, Simulation of global sulfate distribution and the influence on effective cloud drop radii with a coupled photochemistry-sulfur cycle model, *Tellus, Ser. B 50*, 224–242, 1998.

Roelofs, G.-J., et al., Analysis of regional budgets of sulfur species modeled for the COSAM exercise, *Tellus Ser. B, in press*, 2001.

Russell, G.L.,, and A. Lerner, A finite difference scheme

for the tracer transport equation, *J. Appl. Meteorol., 20,* 1483-1498, 1981.

Schwartz, S. E., The whitehouse effect- Shortwave radiative forcing of climate by anthropogenic aerosols, an overview, *J. Aerosol Sci., 27,* 359-382, 1996.

Spiro, P. A., D. J. Jacob, and J. A. Logan, Global inventory of sulfur emissions with 1° x 1° resolution, *J. Geophys. Res., 97,* 6023-6036, 1992.

Tanré, D., M. Herman, and Y. J. Kaufman, Information on aerosol size distribution contained in solar reflected radiances, *J. Geophys. Res., 101,* 19,043-19,060, 1996.

Tegen, I., and I. Fung, Modeling of mineral dust in the atmosphere: Sources, transport, and optical thickness, *J. Geophys. Res., 99,* 22,897-22,914, 1994.

Tegen, I., P. Hollrig, M. Chin, I. Fung, D. Jacob, and J. Penner, Contribution of different aerosol species to the global aerosol extinction optical thickness: Estimations from model results, *J. Geophys. Res., 102,* 23,895-23,915, 1997.

Ten Brink, H. M., C. Kruisz, G. P. A. Kos, and A. Berner, Composition of the light-scattering aerosol in the Netherlands, *Atmos. Environ., 31,* 3955-3962, 1996a.

Ten Brink, H. M., J. P. Veefkind, A. Waaijers-IJpelaan, and J. C. H. van der Hage, Aerosol light-scattering in the Netherlands, *Atmos. Environ., 30,* 4251-4261, 1996b.

Tiedtke, M., A comprehensive mass flux scheme for cumulus parametrization in large scale models, *Mon. Weather Rev., 117,* 1779-1800, 1989.

Tiedtke, M., Representation of clouds in large-scale models, *Mon. Weather Rev., 121,* 3040-3061, 1993.

Veefkind, J. P., Aerosol satellite remote sensing, Ph.D. thesis Univ. of Utrecht, Utrecht, The Netherlands, 1999.

Veefkind, J. P., J. C. H. van der Hage, and H. M. Ten Brink, Nephelometer derived and directly measured aerosol optical depth of the atmospheric boundary layer, *Atmos. Res., 41,* 217-228, 1996.

Veefkind, J. P., G. de Leeuw, and P. A. Durkee, Retrieval of aerosol optical depth over land using two-angle view satellite radiometry during TARFOX, *Geophys. Res. Lett., 25,,* 3135-3138, 1998.

F. Dentener and S. Metzger, Institute for Marine and Atmospheric Research Utrecht (IMAU), Universiteit Utrecht, Princetonplein 5, NL-3508 TA Utrecht, The Netherlands. (e-mail: frank.dentener@jrc.it; S.M.Metzger@phys.uu.nl)

A. Jeuken and J. P. Veefkind, Royal Netherlands Meteorological Institute, Postbus 201, NL-3730 AE, De Bilt, The Netherlands. (e-mail: veefkind@knmi.nl; A.Jeuken@riza.rws.minvenw.nl)

C. Robles Gonzalez, TNO Physics and Electronics Laboratory, PO-Box 96841, NL-2509 JG, The Hague, The Netherlands. (e-mail: robles-gonzalez@fel.tno.nl)